

## Supplementary Information

# Additive-free N-methylation reaction catalyzed by Pt single atoms and clusters on $\alpha$ -MoC synergistically using methanol as a sustainable C1 source

Shurui Fan<sup>a,§</sup>, Mingyuan Zhang<sup>c,§</sup>, Xiangxin Jin<sup>a,b</sup>, Zirui Gao<sup>d</sup>, Yao Xu<sup>d</sup>, Maolin Wang<sup>d</sup>, Chuqiao Song<sup>a,b</sup>, Houhong Song<sup>c</sup>, Xiangxiang Chen<sup>a,b</sup>, Rulong Ma<sup>a</sup>, Siyu Yao<sup>c</sup>, Rui Gao<sup>c\*</sup>, Xiaonian Li<sup>a\*</sup> and Lili Lin<sup>a,b\*</sup>

- a. Institute of Industrial Catalysis, State Key Laboratory of Green Chemistry Synthesis Technology, College of Chemical Engineering, Zhejiang University of Technology, Hangzhou 310014, China.*
- b. Zhejiang Carbon Neutral Innovation Institute & Zhejiang International Cooperation Base for Science and Technology on Carbon Emission Reduction and Monitoring, Zhejiang University of Technology, Hangzhou 310014, China*
- c. College of Chemistry and Chemical Engineering, Inner Mongolia University, Hohhot 010021, China*
- d. Beijing National Laboratory for Molecular Sciences, College of Chemistry and Molecular Engineering, Peking University, Beijing 100871, China*
- e. Key Laboratory of Biomass Chemical Engineering of Ministry of Education, College of Chemical and Biological Engineering, Zhejiang University, Hangzhou 310027, China*

<sup>§</sup>Shurui Fan and Mingyuan Zhang contributed equally.

Corresponding Author

\* Corresponding author's E-mail address: Lili Lin: linll@zjut.edu.cn, xnli@zjut.edu.cn, gaorui@imu.edu.cn

# 1. Experimental section

## 1.1 Catalysts preparation

### 1.1.1 Chemicals and Materials

All chemicals were used as received without further purification.

Chloroplatinic acid hexahydrate (Pt:37.5%+, Shanghai Titan Technology Co., Ltd.), ammonium molybdate tetrahydrate (98%+, Shanghai Titan Technology Co., Ltd.), methanol (anhydrous, AR, Sinopharm Chemical Reagent Co., Ltd.), formic acid (AR, 88%, Sinopharm Chemical Reagent Co., Ltd.), formaldehyde solution (37%-40%, Sinopharm Chemical Reagent Co., Ltd.), quinoline (AR, Sinopharm Chemical Reagent Co., Ltd.), m-xylene (AR, Sinopharm Chemical Reagent Co., Ltd.), *N,N*-Dimethylformamide (AR, Sinopharm Chemical Reagent Co., Ltd.), 1-Propanol (AR, Sinopharm Chemical Reagent Co., Ltd.), acetone (AR, Sinopharm Chemical Reagent Co., Ltd.).

### 1.1.2 Preparation of $\alpha$ -MoC Support

The preparation method of  $\alpha$ -MoC support can be seen in the previous work<sup>1,2</sup>.  $\text{MoO}_3$  was prepared by calcining a certain amount of ammonium paramolybdate  $((\text{NH}_4)_6\text{Mo}_7\text{O}_{24}\cdot 4\text{H}_2\text{O})$  in a muffle furnace to 500 °C and holding at 500°C for 4 hours.

### 1.1.3 Preparation of the catalysts

The 2 wt% Pt/ $\text{Al}_2\text{O}_3$ , 2 wt% Pt/ $\text{TiO}_2$ , and 2 wt% Pt/ $\text{CeO}_2$  catalysts were prepared by impregnation method using  $\text{H}_2\text{PtCl}_6\cdot 6\text{H}_2\text{O}$  as the precursor. In a typical synthesis, 0.3 g of the support was dispersed in 30 mL of deionized water and the oxygen in the round bottom flask was removed by  $\text{N}_2$ . Then the necessary mass of Pt precursor solution was added to the water under vigorous stirring. The mixture was stirred for 3 hours at room temperature under  $\text{N}_2$  atmosphere. The water in the mixture is evaporated by a rotary evaporator at 58°C to obtain a solid sample. The sample was dried overnight in a vacuum freeze dryer to collect catalyst powder. Before catalytic evaluation, the powder (Pt/ $\text{Al}_2\text{O}_3$ , Pt/ $\text{TiO}_2$  and Pt/ $\text{CeO}_2$ ) was subjected to heat treatment at 200 °C using a programmed tubular furnace with the temperature increased at a ramp rate of 5 °C/min and holding at 200 °C for 2 hours under a  $\text{N}_2/\text{H}_2$  mixture (20/80 v/v).

## 1.2 Density function theory calculations

**Calculation Methods:** All structure optimizations and energy calculations are carried out by the density functional theory (DFT) combined with generalized gradient approximation (GGA) for exchange-correlation potential prescribed by Perdew, Burke and Ernzerh (PBE)<sup>3</sup>, implemented in the Vienna ab initio simulation package (VASP)<sup>4,5</sup>. The kinetic energy cutoff of 450 eV is used for wave function expansion. The Self-consistent field (SCF) and force convergence criteria are set to  $1 \times 10^{-4}$  eV and 0.02 eV/Å, respectively.

The adsorption energy ( $E_{\text{ads}}$ ) is calculated as follows:  $E_{\text{ads}} = E_{\text{X/slab}} - (E_{\text{slab}} + E_{\text{X}})$ , where  $E_{\text{X/slab}}$  is the total energy of the system;  $E_{\text{slab}}$ , the energy of the surface; and  $E_{\text{X}}$ , the calculated energy of a molecule in the gas phase. In order to determine the reaction path of the minimum energy, the Climbing image nudged elastic band (CI-NEB) method<sup>6</sup> was used to search the transition state. The energy barrier ( $E_{\text{a}}$ ) and reaction energy ( $\Delta E_{\text{r}}$ ) were calculated according to  $E_{\text{a}} = E_{\text{TS}} - E_{\text{IS}}$  and  $\Delta E_{\text{r}} = E_{\text{FS}} - E_{\text{IS}}$ , where  $E_{\text{IS}}$ ,  $E_{\text{TS}}$  and  $E_{\text{FS}}$  were the energy of initial states, transition states and final states respectively.

**Calculation Models:** The optimized lattice constant of cubic platinum cell (fcc) and cubic MoC cell (fcc) is 3.919 Å and 4.332 Å respectively, which is in good agreement with the experimental results (3.924 Å and 4.270 Å) and the length of Pt-Pt bond and Mo-Mo bond is 2.771 Å and 3.063 Å, respectively. The side-view and top-view of optimized  $\text{Pt}_1/\text{MoC}(111)$  and  $\text{Pt}_4/\text{MoC}(111)$  structures are given in **Figure S15**, which the unit cell is modeled by a  $3 \times 3$  unit and both the two models are sampled by  $3 \times 3 \times 1$  k-point.

Overall, in  $\text{Pt}_1/\text{MoC}(111)$  and  $\text{Pt}_4/\text{MoC}(111)$  structures, the former has 1 Pt atom and the latter has 4 Pt atoms, of which the bottom 36 C atoms and 20 Mo atoms are fixed in  $\text{MoC}(111)$  substrate consisting of 60 C atoms and 60 Mo atoms.

## 2. Figures and Tables

**Table S1.** The platinum loading content of Pt-based catalysts <sup>a</sup>.

Entry	Catalyst	Loading (wt%)
1	0.5 wt% Pt <sub>1</sub> /α-MoC	0.5
2	2 wt% Pt <sub>1+n</sub> /α-MoC	1.9
3	2 wt% Pt <sub>p</sub> /α-MoC	1.9
4	2 wt% Pt/Al <sub>2</sub> O <sub>3</sub>	1.9
5	2 wt% Pt/TiO <sub>2</sub>	2.0
6	2 wt% Pt/CeO <sub>2</sub>	1.9

<sup>a</sup>: The metal contents of the catalyst were measured by Inductively Coupled Plasma Optical Emission Spectrometry (ICP-OES).

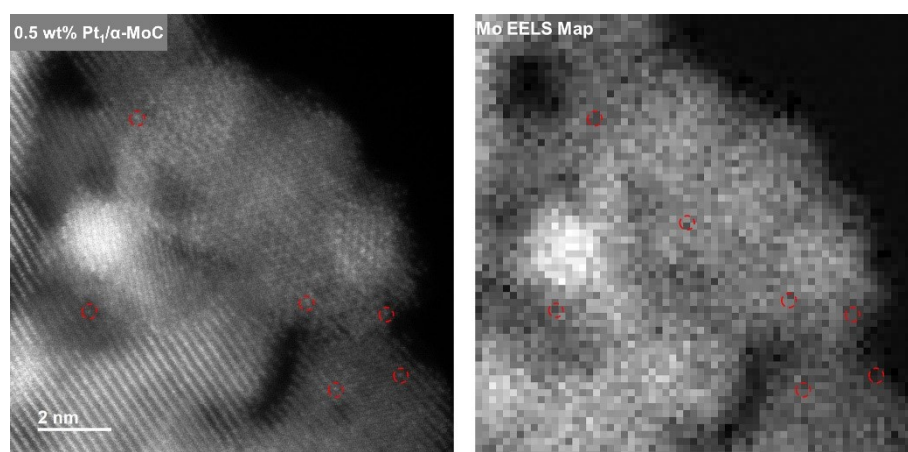


**Figure S1.** HAADF-STEM image and Mo EELS map of Pt<sub>1</sub>/α-MoC. Pt single atoms are marked with small red circles.

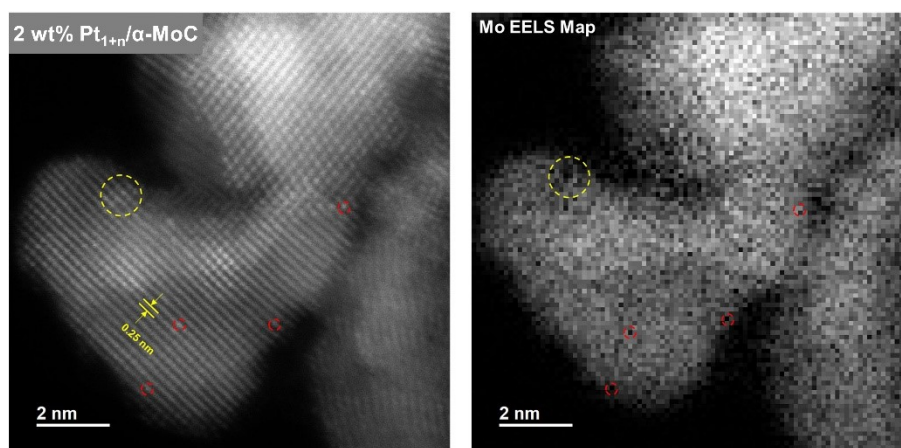


**Figure S2.** HAADF-STEM image and Mo EELS map of Pt<sub>1+n</sub>/α-MoC. Pt single atoms are marked with small red circles, and Pt clusters are marked with slightly larger yellow circles.

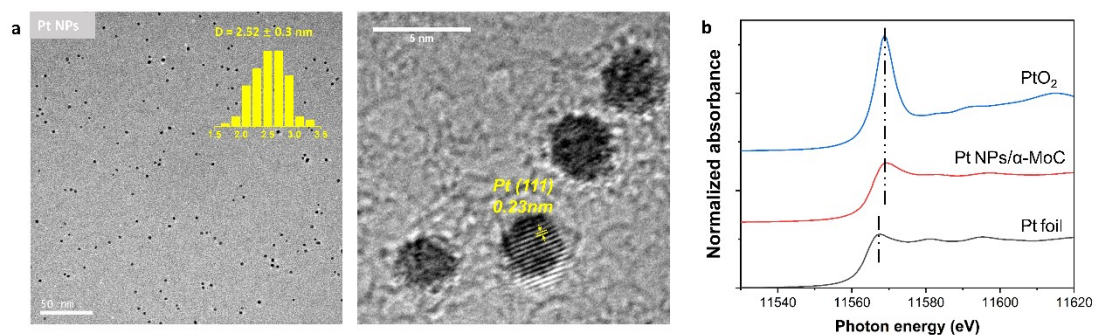


**Figure S3.** (a) TEM images of the PVP-Pt NPs. The average particle size of Pt nanoparticles is 2.52 nm. (b) Molybdenum K-edge (20,000 eV) X-ray absorption near-edge structure (XANES) spectra of Pt NPs/α-MoC catalyst, molybdenum foil and molybdenum oxides. The Pt NPs/α-MoC catalyst was not activated by CH<sub>4</sub>/H<sub>2</sub> mixed atmosphere.

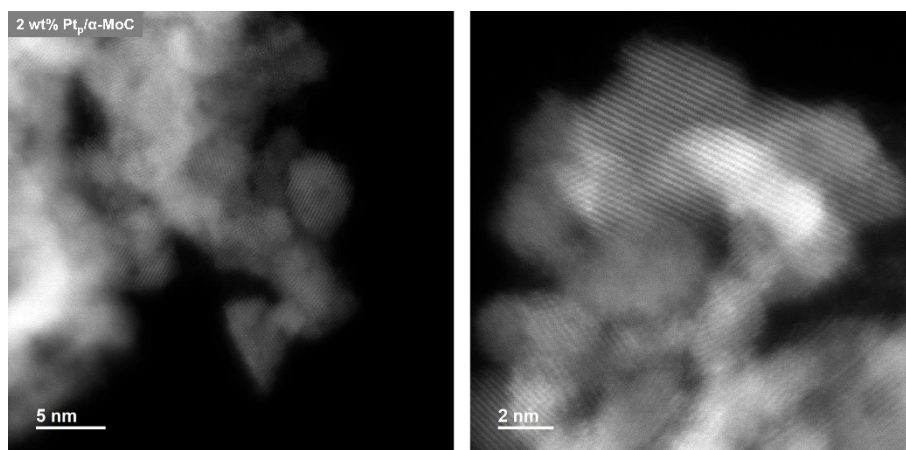


**Figure S4.** HAADF-STEM image of  $\text{Pt}_p/\alpha\text{-MoC}$ .

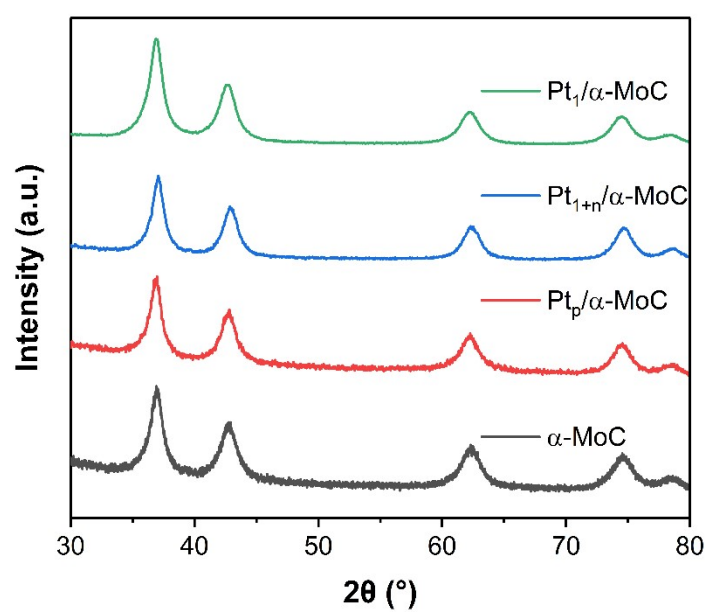


**Figure S5.** XRD patterns of the  $\text{Pt}_1/\alpha\text{-MoC}$ ,  $\text{Pt}_{1+n}/\alpha\text{-MoC}$ ,  $\text{Pt}_p/\alpha\text{-MoC}$  and the  $\alpha\text{-MoC}$  support.

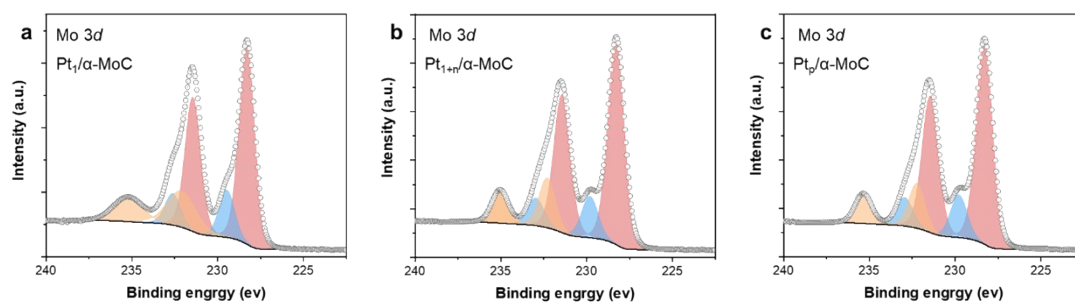


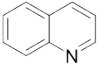
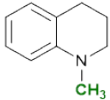
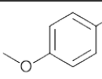
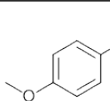
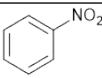
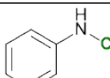
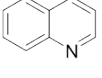
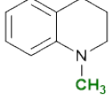
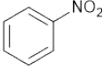
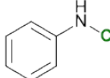
**Figure S6.** Mo 3d XPS spectrum of (a) Pt<sub>1</sub>/α-MoC; (b) Pt<sub>1+n</sub>/α-MoC; (c) Pt<sub>p</sub>/α-MoC.

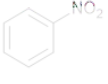
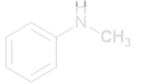
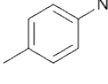
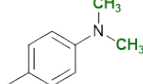
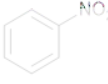
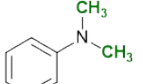
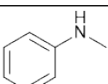
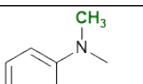
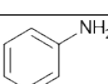
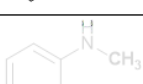
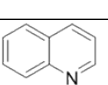
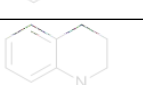
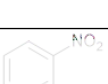
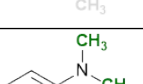
**Table S2.** Curve-fit Parameters <sup>a</sup> for Pt L3-edge EXAFS of Pt/α-MoC catalysts.

Catalysts	Shell	d(Å) <sup>b</sup>	Coordination number <sup>c</sup>	ΔE <sub>0</sub> (eV)	σ <sup>2</sup> (Å <sup>2</sup> ) <sup>d</sup>
0.5% Pt <sub>1</sub> /α-MoC	Pt-O/C	1.94 ± 0.03	1.6 ± 0.3	3 ± 1	0.007 ± 0.003
	Pt-Mo	2.89 ± 0.01	2.9 ± 0.8		0.009 ± 0.002
2% Pt <sub>1+n</sub> /α-MoC	Pt-Mo	2.73 ± 0.02	2.0 ± 0.6	5 ± 1	0.006 ± 0.001
	Pt-Pt	2.75 ± 0.01	5.2 ± 0.9		0.005 ± 0.002
2% Pt <sub>p</sub> /α-MoC	Pt-Pt	2.73 ± 0.01	6.9 ± 0.6	4 ± 1	0.006 ± 0.001
	Pt-Mo	2.74 ± 0.01	1.0 ± 0.2		0.002 ± 0.001

*a:* The data ranges used in the fit are  $3.0 \leq k \leq 12.0 \text{ \AA}^{-1}$  and  $1.0 \sim 1.2 \leq R \leq 3.0 \sim 3.5 \text{ \AA}$ .  $S_0^2$  was fixed at 0.737, obtained from the Pt foil measured at the same time. The numbers of variable parameters are out of the total of independent data points. *R*-factors for these fittings are all below 0.017. *b:* The half path length. The paths for Pt-O, Pt-Mo and Pt-Pt are from the crystal structure of PtO<sub>2</sub> (P6<sub>3</sub>mc, ICSD 24923), MoPt (Pmma, ICSD 644160) and Pt (Fm-3m, ICSD 180981). *c:* average coordination number. *d:* Debye-Waller factor.

**Table S3.** Reductive *N*-methylation reactions under different catalytic systems

	Heterogeneous catalyst	Temp./ Time	C1/Hydrogen source	Additive	Substrate	Product	Yield (%)
Ref. 1 <sup>7</sup>	10% Pd/C+Zn	150 °C / 40 h	Methanol/H <sub>2</sub> O	1.5eq. Zn			75
Ref. 2 <sup>8</sup>	5% Fe <sub>2</sub> O <sub>3</sub> /Gr@C	130 °C / 30 h	Paraformaldehyde	2eq. Na <sub>2</sub> CO <sub>3</sub>			86
Ref. 3 <sup>9</sup>	4% Ir@YSMCN	170 °C / 30 h	Methanol	1eq. <i>t</i> -BuOK			97
Ref. 4 <sup>10</sup>	2.5% Pd/C	100 °C / 12 h	Paraformaldehyde/ 1 MPa H <sub>2</sub>	-			98
Ref. 5 <sup>11</sup>	1% Pt/C	150 °C / 24 h	Methanol/ 0.2 MPa H <sub>2</sub>	1eq. <i>t</i> -BuOK			92

Ref. 6 <sup>12</sup>	5% Pd/C	130 °C / 20 h	Methanol	4eq. <i>t</i> -BuOK			92
Ref. 7 <sup>13</sup>	27% Cu/Al <sub>2</sub> O <sub>3</sub>	130 °C / 15 h	Paraformaldehyde	2eq. Na <sub>2</sub> CO <sub>3</sub>			97
Ref. 8 <sup>14</sup>	4% Co <sub>3</sub> O <sub>4</sub> /NGr@C	100 °C / 24 h	Formaldehyde/formic acid	~29eq. <i>t</i> -BuOH			80
Ref. 9 <sup>15</sup>	Pd-ZnO/TiO <sub>2</sub>	180 °C / 24 h	1.5 MPa CO <sub>2</sub> / 4.5 MPa H <sub>2</sub>	-			94 <sup>a</sup>
Ref. 10 <sup>16</sup>	10% Ag/Al <sub>2</sub> O <sub>3</sub>	230 °C / 24 h	3 MPa CO <sub>2</sub> / 3 MPa H <sub>2</sub>	-			90 <sup>a</sup>
This work	2% Pt <sub>1+n</sub> /α-MoC	190 °C / 3 h	Methanol	-			98
		190 °C / 5 h					95

a. *N*-methylation of aniline

The results of the reductive *N*-methylation reactions of different catalytic systems reported were summarized as shown in Table S3. In comparison to the catalytic systems presented in the table, the catalyst prepared in this work demonstrates significant advantages, as it is capable of achieving excellent yields of the corresponding *N*-methyl product merely in a methanol aqueous solution without additives or molecular hydrogen. It should be noted that CO<sub>2</sub> is often used as a C1 source for the *N*-methylation of aniline compounds rather than that of reductive *N*-methylation reactions of nitrobenzene.



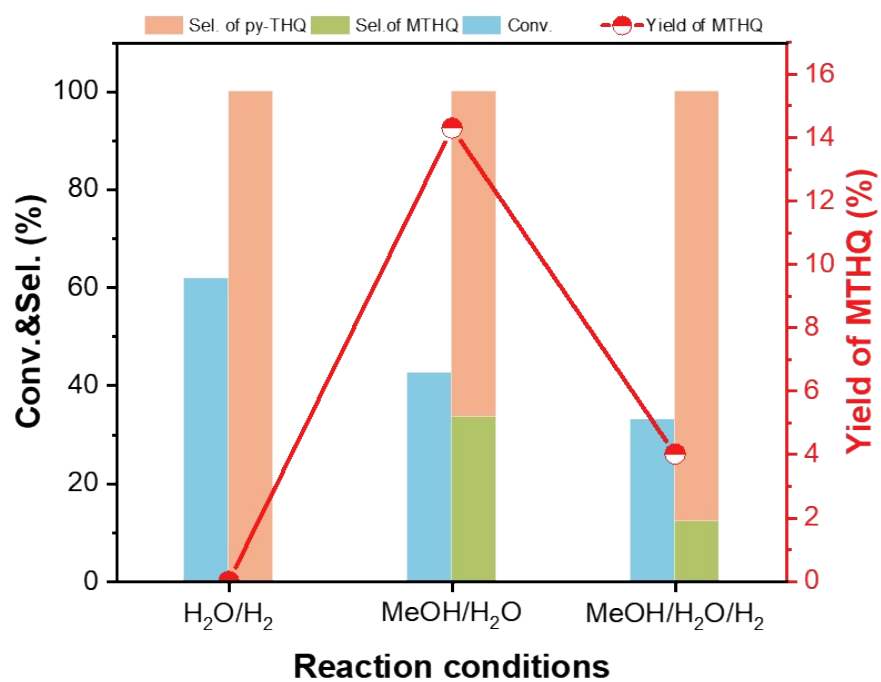


**Figure S7.** Catalytic performance of Pt/α-MoC catalysts in the reductive *N*-methylation of quinolone under different condition. Reaction conditions: 25 mg Pt/α-MoC, 15 mL (H<sub>2</sub>O or MeOH: H<sub>2</sub>O = 9:1), 1 mmol quinoline, 0.3 MPa N<sub>2</sub>, 3h.

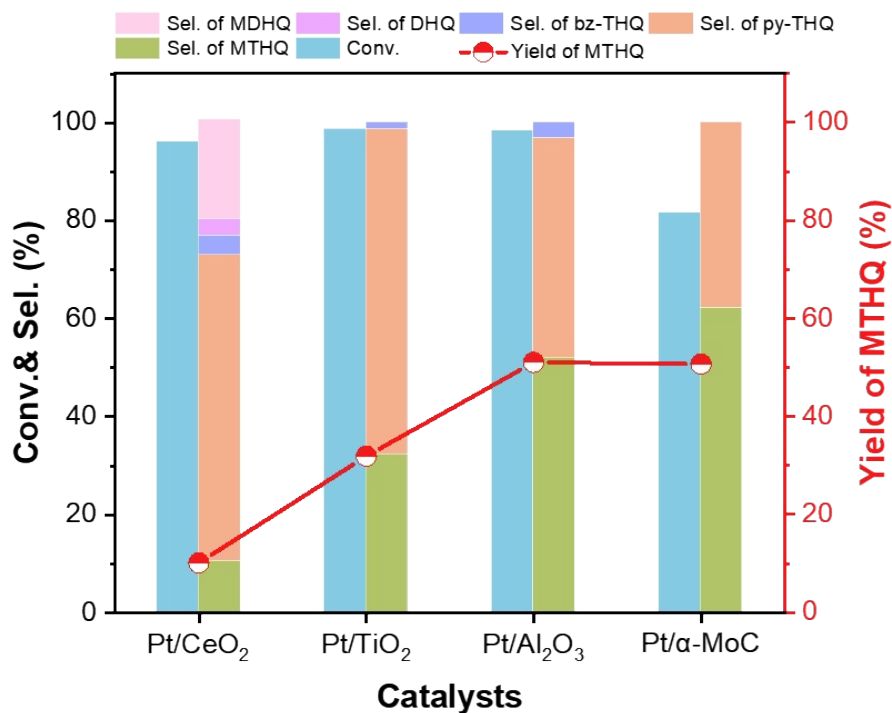


**Figure S8.** Effect of different supports under H<sub>2</sub> atmosphere. Reaction conditions: 100 mg of catalyst, 15 mL MeOH, 1 mmol quinoline, 1 MPa H<sub>2</sub>, 3h, 190 °C. Abbreviation: bz-THQ represents 5,6,7,8-tetrahydroquinoline, and DHQ represents decahydroquinoline, and MDHQ represents 1-methyldecahydroquinoline.

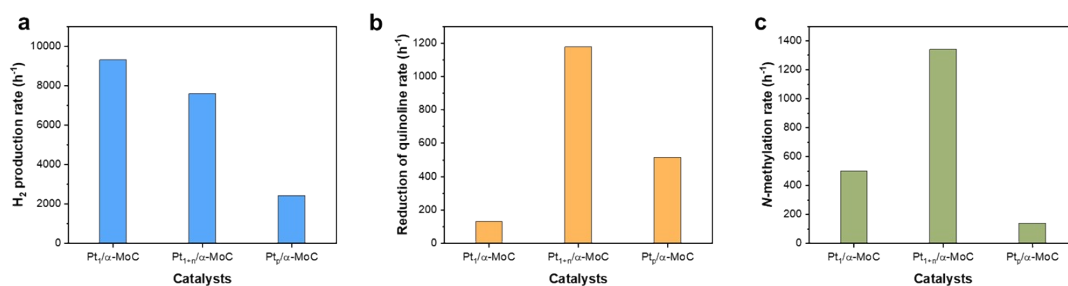


**Figure S9.** Activity of various Pt/α-MoC on the hydrogen production from aqueous phase methanol reforming (APRM), reduction of *N*-heteroarene and the *N*-methylation of the py-THQ with methanol. Reaction conditions: 25 mg catalysts, 15 mL MeOH/H<sub>2</sub>O, 1 mmol quinoline, 0.3 MPa N<sub>2</sub>.

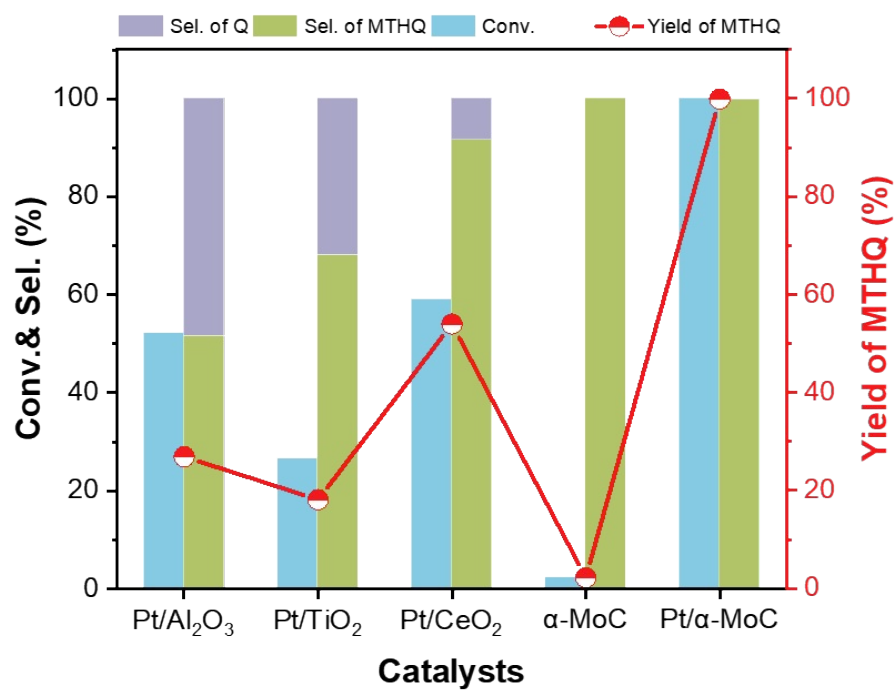


**Figure S10.** Catalytic performance of Pt catalysts in the *N*-methylation reaction of py-THQ. Reaction conditions: 100 mg of catalyst, 15 mL MeOH/H<sub>2</sub>O, 1 mmol py-THQ, 0.3 MPa N<sub>2</sub>, 3h, 190 °C.

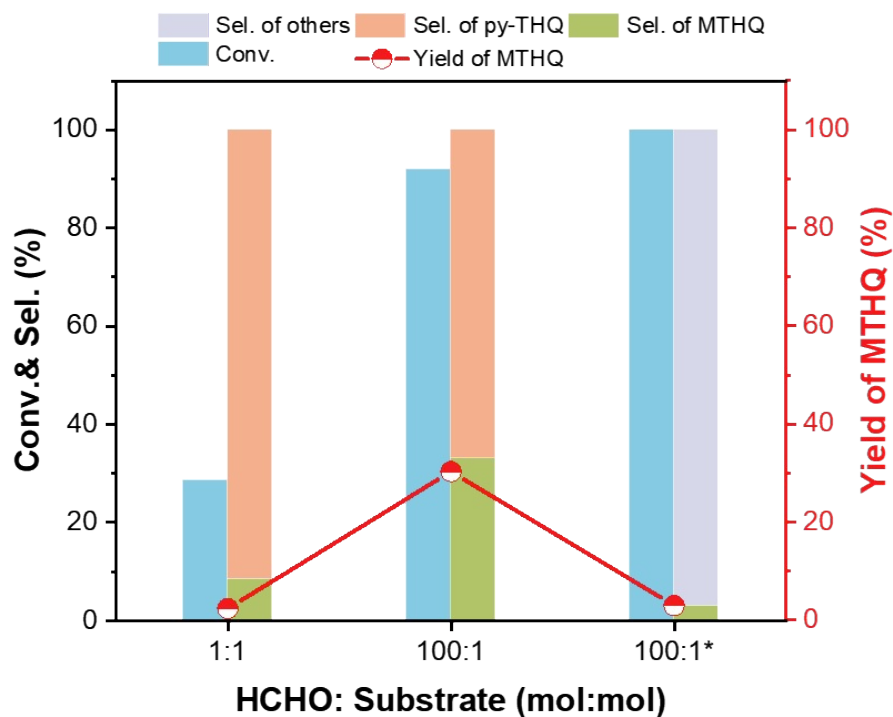


**Figure S11.** Effects of different methylation reagents. Others: 15.1% of 3-ethyl-1,2,3,4-tetrahydroquinoline, 76.5% of 2,4,8-trimethyl-1,2,3,4-tetrahydroquinoline, 5.4% of 2,2,4,8-tetramethyl-1,2,3,4-tetrahydroquinoline. Reaction conditions: 100 mg  $Pt_{1+n}/\alpha$ -MoC, 15 mL  $HCHO/H_2O$ , 1 mmol quinolone (\*: 1 mmol py-THQ), 0.3 MPa  $N_2$ , 3h, 190 °C.

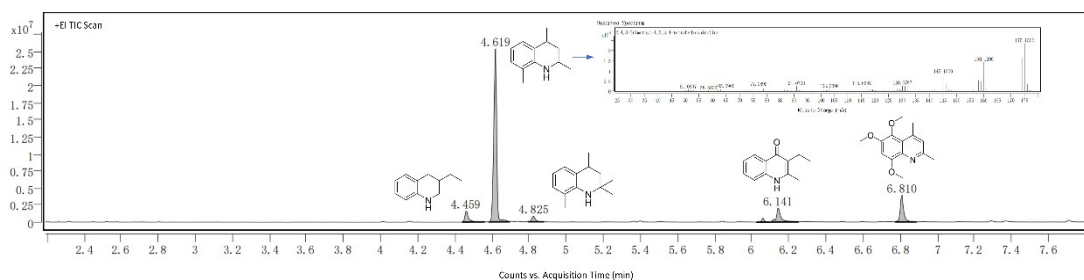


**Figure S12.** The GC-MS spectrum for the  $Pt_{1+n}/\alpha$ -MoC catalyzed reductive *N*-methylation of quinoline using formaldehyde as C1 source.

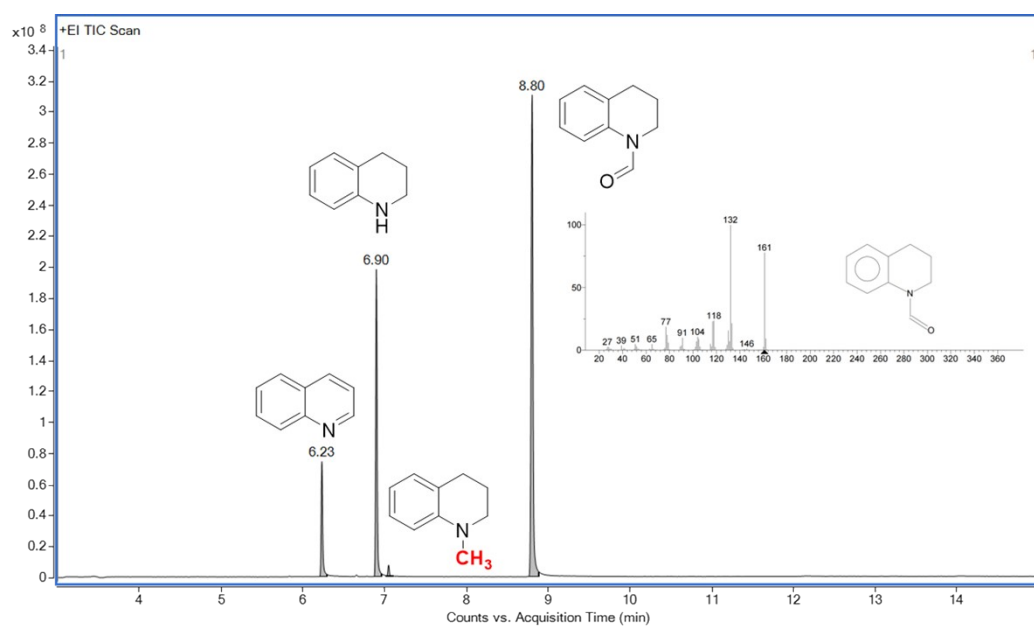


**Figure S13.** The GC-MS spectrum for the Pt<sub>1+n</sub>/α-MoC catalyzed reductive *N*-methylation of quinoline using formic acid as C1 source.

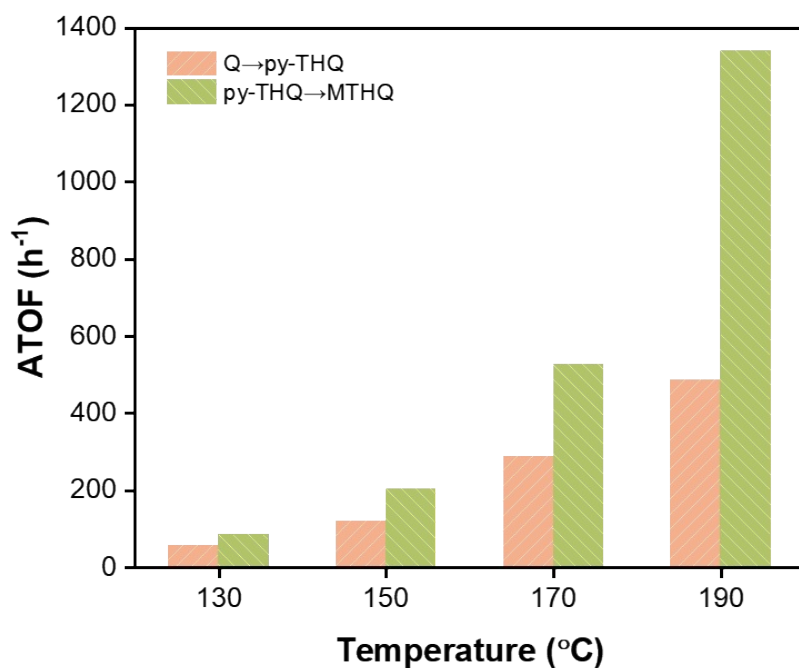


**Figure S14.** Effect of reaction temperature on Pt<sub>1+n</sub>/α-MoC catalyst. Reaction conditions: 25 mg Pt<sub>1+n</sub>/α-MoC, 15 mL CH<sub>3</sub>OH/H<sub>2</sub>O (9:1, molar ratio), 5 mmol quinolone, 0.3 MPa N<sub>2</sub>, 190 °C. Reaction conversion is controlled in the kinetic range by adjusting the reaction time, less than 15%.

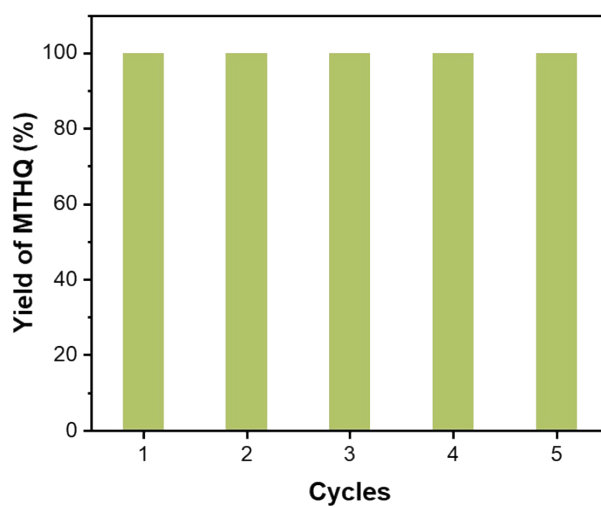
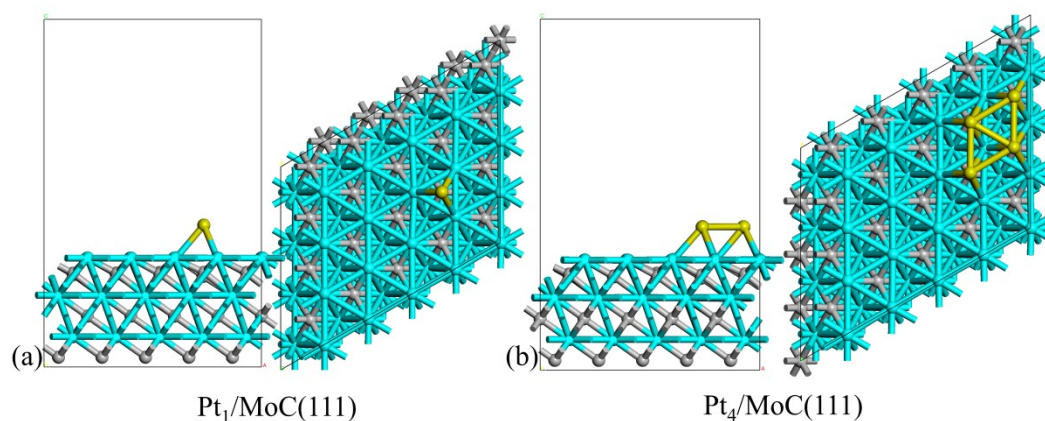


**Figure S15.** Recyclability evaluation of Pt<sub>1+n</sub>/α-MoC catalyst for the reductive *N*-methylation of quinoline in successive runs. Reaction conditions: 100 mg Pt<sub>1+n</sub>/α-MoC, 15 mL MeOH/H<sub>2</sub>O, 1 mmol quinoline, 0.3 MPa N<sub>2</sub>, 3 h, *m*-Xylene as internal standard, yields were determined by GC.

**Table S4.** The mass fraction of Pt in different samples.

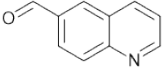
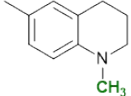
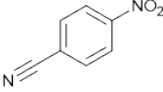
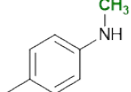
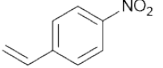
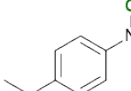
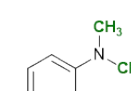
Entry	The mass fraction of Pt (%) <sup>a</sup>
Pt <sub>1+n</sub> /α-MoC-fresh	1.9
Pt <sub>1+n</sub> /α-MoC-cycle-5 <sup>th</sup> <sup>b</sup>	1.9
Liquid products after reaction	<0.0001

*a. The results were measured by ICP-OES; b. the catalyst was collected after the fifth cycle.*



**Figure S16.** Surface Model. Side-view and top-view of optimized structures of a) Pt<sub>1</sub>/ MoC(111) and b) Pt<sub>4</sub>/MoC(111). (Mo/cyan; C/gray; Pt/yellow)

**Table S5.** The reductive N-methylation of quinolines and nitroarenes functionalized with reducible groups over Pt<sub>1+n</sub>/α-MoC <sup>a</sup>.

Entry	Substrate	Product	Temp. (°C)	Time (h)	Conv. (%) <sup>b</sup>	Sel. (%) <sup>b</sup>
1			190	3	99.9	62.7
2			150	3	99.9	71.6
3		 / 	150	3	99.9	68.0 / (24.1)

<sup>a</sup> Reaction conditions: 50mg of catalyst, 0.25 mmol of a substrate, 15 mL methanol/H<sub>2</sub>O, 0.3 MPa N<sub>2</sub>;

<sup>b</sup> Identified by GC-MS.

## Reference:

- 1 L. Lin, W. Zhou, R. Gao, S. Yao, X. Zhang, W. Xu, S. Zheng, Z. Jiang, Q. Yu, Y. W. Li, C. Shi, X. D. Wen and D. Ma, *Nature*, 2017, **544**, 80–83.
- 2 L. Lin, S. Yao, R. Gao, X. Liang, Q. Yu, Y. Deng, J. Liu, M. Peng, Z. Jiang, S. Li, Y. W. Li, X. D. Wen, W. Zhou and D. Ma, *Nat. Nanotechnol.*, 2019, **14**, 354–361.
- 3 J. P. Perdew, K. Burke and M. Ernzerhof, *Phys. Rev. Lett.*, 1996, **77**, 3865–3868.
- 4 G. Kresse and J. Furthmüller, *Comput. Mater. Sci.*, 1996, **6**, 15–50.
- 5 G. Kresse and J. Furthmüller, *Phys. Rev. B*, 1996, **54**, 11169–11186.
- 6 G. A. Henkelman, B. P. Uberuaga and H. Jónsson, *J. Chem. Phys.*, 2000, **113**, 9901–9904.
- 7 B. Abarca, R. Adam and R. Ballesteros, *Org. Biomol. Chem.*, 2012, **10**, 1826–1833.
- 8 K. Natte, H. Neumann, R. V. Jagadeesh and M. Beller, *Nat. Commun.*, 2017, **8**, 1–9.
- 9 A. Fu, Q. Liu, M. Jiang and G. Xu, *Asian J. Org. Chem.*, 2019, **8**, 487–491.
- 10 H. Wang, Y. Huang, Q. Jiang, X. Dai and F. Shi, *Chem. Commun.*, 2019, **55**, 3915–3918.
- 11 M. A. R. Jamil, A. S. Touchy, M. N. Rashed, K. W. Ting, S. M. A. H. Siddiki, T. Toyao, Z. Maeno and K. ichi Shimizu, *J. Catal.*, 2019, **371**, 47–56.
- 12 V. Goyal, J. Gahtori, A. Narani, P. Gupta, A. Bordoloi and K. Natte, *J. Org. Chem.*, 2019, **84**, 15389–15398.
- 13 X. Dong, Z. Wang, Y. Yuan and Y. Yang, *J. Catal.*, 2019, **375**, 304–313.
- 14 T. Senthamarai, K. Murugesan, K. Natte, N. V. Kalevaru, H. Neumann, P. C. J. Kamer and R. V. Jagadeesh, *ChemCatChem*, 2018, **10**, 1235–1240.
- 15 W. Lin, H. Cheng, Q. Wu, C. Zhang, M. Arai and F. Zhao, *ACS Catal.*, 2020, **10**, 3285–3296.
- 16 Y. Long, J. He, H. Zhang, Y. Chen, K. Liu, J. Fu, H. Li, L. Zhu, Z. Lin, A. Stefancu, E. Cortes, M. Zhu and M. Liu, *Chem. - A Eur. J.*, , DOI:10.1002/chem.202203152.